9-13 (bromide) and 7-11 (chloride) in support of the above notion.

The fact that the B bands, which correspond to transitions from the $S = 2$ ground level, appear at lower energy than the A bands, which originate in the $S = 1$ level, indicates that J_{eff}' is smaller than J_{gs}. A similar situation was found for the $^4T_1(G)$ state in $KMg_{1-x}Mn_xF_3$.[6] Care is necessary, however, with this interpretation because, strictly speaking, $J_{eff}'(^4T_2)$ is not defined, since an operator of the form (3) does not apply.

Bands 7, 11, and 12 (bromide) deserve special comment. Their decrease in size between 2 and 8 K is compatible only with their assignment as pair transitions originating in the $S = 0$ ground level. (Bands 11 and 12 appear to overlay single-ion absorptions as well.) Since the excited-state spin quantum numbers range from 1 to 4, these bands correspond to $\Delta S = 1$ transitions. Band 7 is 14.5 cm^{-1} higher in energy than band 5, which corresponds to a $\Delta S = 0$ transition originating in the $S = 1$ ground level. Since 14.2 cm^{-1} is the calculated energy of the singlet-triplet separation in the ground state, both transitions 5 and 7 are likely to lead to the same excited level. The occurrence of $\Delta S = 1$ excitations is not surprising when one considers the fact that in this singly excited pair state S is no longer a sharply defined quantum number as a result of spin-orbit coupling.

The observation of Zeeman effects in the $^4T_2(D)$ single pair excitations of the bromide complex can be explained as follows: in contrast to the case of $^4A_1$, the g values in the $^4T_2$ state deviate from 2.0 due to some orbital contributions. This leads to different Zeeman splittings of ground and excited states and thus effective Zeeman splittings even for $\Delta M_S = 0$ as well as $\Delta M_S = \pm 1$ transitions.

$^4E(D)$ Singly Excited State. The region of $^4E(D)$ transitions in the bromide provides a particularly fine example of a pair spectrum. The bands 1 and 2 (Figure 10) have the same temperature dependence as the A bands in the $^4A_1$ and $^4T_2$ regions. From this we can assign them to transitions originating in the $S = 1$ ground level. The energy difference between bands 1 and 2 corresponds to an excited-state splitting. It is most likely a result of the combined effects of spin-orbit coupling and trigonal crystal field, which are expected to produce a second-order splitting of the order of a few wave numbers.[4] Bands 3 and 4 are identified from their temperature dependence as cold pair bands originating in the $S = 0$ pair level. They are displaced from bands 1 and 2 by 14.0 cm^{-1}, the singlet-triplet separation of the ground state. The corresponding energy level diagram including the observed transitions is shown in Figure 10. Bands 5 and 6 are probably single-ion transitions to two spin-orbit components of ^4E.

We have not observed any $2 \rightarrow 2$ pair transition for this state. At the highest temperature used (ca. 20 K) the corresponding bands are expected to be still rather weak. And if they lie at higher energy than the $1 \rightarrow 1$ bands, as was the case for $KMg_{1-x}Mn_xF_3$,[6] they could lie beneath the other more intense bands observed in this region.

The chloride spectrum is much less resolved in this region. Between 19.8 and 1.4 K a band at 27 794 cm^{-1} decreases sharply in size and vanishes at 1.4 K. We therefore assign it to a pair transition originating in the $S = 1$ level. A weak band lying 21 cm^{-1} higher in energy is assigned to a pair transition originating in the $S = 0$ level. This energy difference (21 cm^{-1}) is in good agreement with a J_{gs} value of 19.6 cm^{-1} determined from the temperature dependence of the $^4A_1$ pair excitations. A third peak lies at 27 837 cm^{-1}, and it is relatively insensitive to temperature in the range studied. It probably represents a single-ion transition.

We have then, through the use of high-resolution absorption and Zeeman spectroscopy, identified manganese(II) pair excitations in $CsMg_{1-x}Mn_xX_3$ (X = Br, Cl) to the singly excited $^4A_1(G)$, $^4T_2(D)$, and $^4E(D)$ states. A full analysis has been carried out only for the $^4A_1$ pair transitions. For the other two orbitally degenerate, singly excited states a simple theoretical model is not yet available.

Acknowledgment. We thank the Swiss National Science Foundation for support (Grant No. 2.427-0.79) and Naomi Furer for preparing the crystals used in this study.

Registry No. $CsMnBr_3$, 36482-50-5; $Mn_2Br_9^{5-}$, 88780-80-7; $Mn_2Cl_9^{5-}$, 58396-13-7.

Contribution from the Department of Chemistry, McMaster University, Hamilton, Ontario L8S 4M1, Canada

^{199}Hg NMR Study of the Hg^{2+}, Hg_2^{2+}, Hg_3^{2+}, and Hg_4^{2+} Cations: The First Example of Hg-Hg Spin-Spin Coupling

RONALD J. GILLESPIE, PIERRE GRANGER,[1] KEITH R. MORGAN, and GARY J. SCHROBILGEN*

Received June 7, 1983

The mercury cations Hg^{2+}, Hg_2^{2+}, Hg_3^{2+}, and Hg_4^{2+} have been studied by ^{199}Hg NMR spectroscopy. For Hg^{2+} and Hg_2^{2+} well-resolved resonances were observed over a wide range of temperatures. For Hg_3^{2+}, only at temperatures less than -40 °C were resonances sufficiently sharp to be observed, and at no temperature down to -70 °C were sharp ^{199}Hg resonances observed in solutions of Hg_4^{2+}. The ^{199}Hg NMR spectra of Hg_3^{2+} show second-order effects due to coupled mercury atoms, and a value for $J_{^{199}Hg-^{199}Hg}$ of 139 600 Hz was obtained, representing the first Hg-Hg and largest nuclear spin-spin coupling constant reported to date.

Introduction

The homopolyatomic cations of mercury can be prepared by oxidation of elemental mercury with a pentafluoride, MF_5 (M = As or Sb), or with Hg^{2+} cation in a suitably weakly basic solvent medium such as SO_2 to give successively Hg_2^{2+}, Hg_3^{2+}, Hg_4^{2+},[2,3] and the linear-chain metallic compounds $Hg_{3-\delta}MF_6$.[4,5] The resulting SO_2-soluble cations Hg_2^{2+}, Hg_3^{2+}, and Hg_4^{2+} and the insoluble linear-chain metallic compounds $Hg_{2.85}AsF_6$ and $Hg_{2.91}SbF_6$ have all been characterized in the solid state

(1) Present address: Département de Chimie, IUT de Rouen, 76130 Mont-Saint-Aignan, France.

(2) Davies, C. G.; Dean, P. A. W.; Gillespie, R. J.; Ummat, P. K. *J. Chem. Soc. D* **1971**, 782.
(3) Cutforth, B. D.; Gillespie, R. J.; Ireland, P. R. *J. Chem. Soc., Chem. Commun.* **1973**, 723.
(4) Cutforth, B. D.; Davies, C. G.; Dean, P. A. W.; Gillespie, R. J.; Ireland, P. R.; Ummat, P. K. *Inorg. Chem.* **1979**, *12*, 1343.
(5) Gillespie, R. J.; Ummat, P. K. *J. Chem. Soc. D* **1971**, 1168.

0020-1669/84/1323-0887$01.50/0

Table I. ^{199}Hg NMR Chemical Shifts for the Hg^{2+}, Hg_2^{2+}, Hg_3^{2+}, and Hg_4^{2+} Cations

solute	solvent	$\delta_{^{199}Hg}$, ppm[a]
$Hg(ClO_4)_2$	H_2O	−2284[c]
$Hg(ClO_4)_2$	H_2O (satd)	−2270
$Hg(ClO_4)_2$	H_2O	−2254[d]
$Hg(AsF_6)_2$	SO_2	−2090
$Hg_2(AsF_6)_2$	SO_2	−2030
$Hg_2(SO_3F)_2$	HSO_3F[b]	−1939
$Hg_2(ClO_4)_2$	H_2O (satd)	−1614[e]
$Hg_2(ClO_4)_2$	H_2O	−1500[d,f]
$Hg_3(AsF_6)_2$[g]	SO_2[b]	−1968[i]
		−965[j]
$Hg_3(SO_3F)_2$[h]	HSO_3F[b]	−1832[i]
		−895[j]
$Hg_4(AsF_6)_2$	SO_2	−1310

[a] Mercury-199 chemical shifts were referenced with respect to neat $(CH_3)_2Hg$ at room temperature. The chemical shift sign convention is that outlined by IUPAC (*Pure Appl. Chem.* **1972**, *29*, 627; **1976**, *45*, 217); i.e., a positive sign signifies a chemical shift to high frequency of the reference compound and vice versa. All chemical shift measurements are at room temperature (24 °C) and are from this work unless otherwise indicated. [b] Spectrum recorded at −70 °C. [c] Reference 4. [d] Reference 5. [e] Chemical shift is concentration dependent. [f] Chemical shift extrapolated to infinite dilution. [g] $J_{^{199}Hg-^{199}Hg} = 139\,700 \pm 300$ Hz. [h] $J_{^{199}Hg-^{199}Hg} = 139\,600 \pm 1000$ Hz. [i] Central mercury atom. [j] Terminal mercury atoms.

by X-ray crystallography.[3,5,6] The compounds $Hg_{2.85}AsF_6$ and $Hg_{2.91}SbF_6$ disproportionate on contact with SO_2 below −20 °C with the formation of metallic mercury and a solution of Hg_4^{2+}. The Hg_4^{2+} cation, itself, is not completely stable in SO_2 solution, disproportionating to the solid metallic compound and Hg_3^{2+}. The present work describes our studies of mercury cations by ^{199}Hg NMR spectroscopy. Mercury-199, which has a spin $I = {}^1/_2$ and occurs at 16.84% natural abundance, has a sensitivity relative to natural-abundance ^{13}C of 5.42. Its high resonance frequency (Ξ = 17.910841 MHz for $(CH_3)_2Hg$ relative to protons in $(CH_3)_4Si$ resonating at precisely 100 MHz), favorable sensitivity, and nonquadrupolar spin make ^{199}Hg particularly suited to study by FT NMR spectroscopy.

Results and Discussion

Hg^{2+} and Hg_2^{2+}. We have measured the chemical shifts of the Hg^{2+} ion in solutions of $Hg(AsF_6)_2$ in SO_2 and of $Hg(ClO_4)_2$ in aqueous solution. These results together with the results of some previous measurements on Hg(II) compounds are summarized in Table I. The value we obtained for the chemical shift of $Hg(ClO_4)_2$ in aqueous solution compares favorably with those reported by previous workers. It has been noted[7] that the shielding of mercury increases from the most covalent compounds such as $Hg(CH_3)_2$ to ionic compounds such as $Hg(ClO_4)_2$, which is consistent with a strong paramagnetic contribution to the chemical shift. However, the chemical shift of the compound $Hg(AsF_6)_2$ in SO_2 does not follow this trend as it is more deshielded than the perchlorate despite the fact that SO_2 is a more weakly coordinating solvent than water.

The only previous studies on Hg_2^{2+} salts by Kruger et al.[8] have been of $Hg_2(ClO_4)_2$ and $Hg_2(NO_3)_2$ in aqueous media. Solutions of $Hg_2(AsF_6)_2$ in SO_2 show a single line between 0 and −60 °C at −2030 ppm. In aqueous solution our value for the chemical shift of the perchlorate, which shows some concentration dependence, is in agreement with that obtained by Kruger et al. (Table I) and shows the perchlorate to be more deshielded, which is consistent with strongly coordinated water molecules.

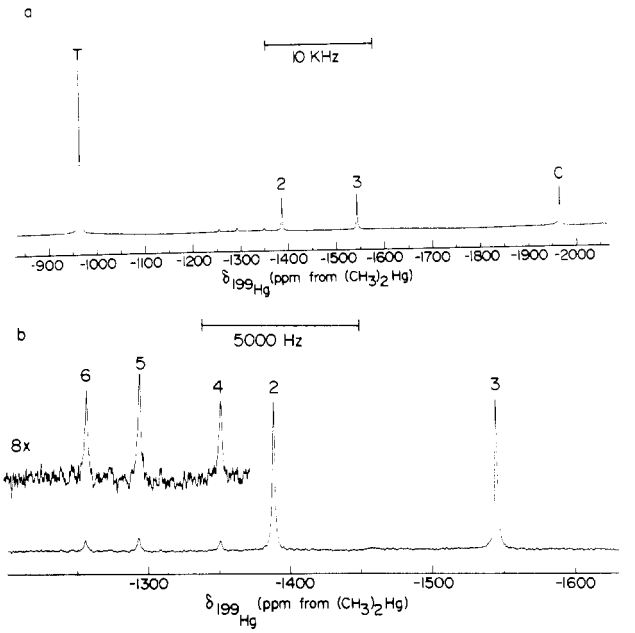

Figure 1. Natural-abundance ^{199}Hg NMR spectrum (44.800 MHz) of the Hg_3^{2+} cation (AsF_6^- salt) dissolved in SO_2 solvent (−70 °C). The individual lines are assigned as follows: (a) ^{199}Hg–Hg–Hg + ^{199}Hg–Hg–^{199}Hg (T), Hg–^{199}Hg–Hg (C), transitions 2 and 3 arise from the AB spin system ^{199}Hg–^{199}Hg–Hg; (b) transitions 4, 5, and 6 arise from the AB_2 spin system ^{199}Hg–^{199}Hg–^{199}Hg; transitions 2 and 3 arise from the AB spin system ^{199}Hg–^{199}Hg–Hg (see ref 10 for schemes used in numbering transitions).

Hg_3^{2+}. Solutions of $Hg_3(AsF_6)_2$ in SO_2 show no discernible ^{199}Hg resonances at room temperature, but when the solution is cooled, broad peaks start to appear at ∼−40 °C. At −60 °C the spectrum depicted in Figure 1a is observed. The two most intense peaks have an intensity ratio of ∼2.5:1. An accurate determination was not possible due to the large spectral width needed to record the whole spectrum. On the basis of this intensity ratio, the more intense peak at −965 ppm was assigned to the terminal mercury atoms and the less intense peak at −1968 ppm to the central mercury atom of Hg_3^{2+} (theoretical ratio 2.40:1). As expected, the terminal mercury atoms are more deshielded since formally the positive charge resides on the terminal mercury atoms and thus they have a smaller bond-order, charge-density term

$$\sum_B Q_{AB}$$

than the central mercury atom in the equation for the paramagnetic contribution to the chemical shift (eq 1).[9] In this

$$\sigma_A^p = \frac{-\mu_0 e^2 h^2 \langle r^{-3} \rangle_p}{8\pi m^2 \Delta E} \sum_B Q_{AB} \qquad (1)$$

equation σ_A^p is the paramagnetic contribution to the chemical shift, $\langle r^{-3} \rangle_p$ is the mean radial factor of the valence p orbital, and ΔE is the mean excitation energy. The two inner peaks of equal intensity were shown to have different chemical shifts when recorded at different applied field strengths, i.e., 2.114 and 5.872 T. These peaks arise from the statistically small amount of Hg_3^{2+} (4.72%) having two adjacent spin-$^1/_2$ ^{199}Hg nuclei and are assigned to the two most intense transitions 2 and 3 of an AB spin system (the numbering scheme used for individual transitions is that given in ref 10). From the two

(6) Brown, D.; Cutforth, B. D.; Davies, C. G.; Gillespie, R. J.; Ireland, P. R.; Vekris, J. E. *Can. J. Chem.* **1974**, *52*, 791.
(7) Sens, M. A.; Wilson, N. K.; Ellis, P. D.; Cook, J. D. *J. Magn. Reson.* **1975**, *19*, 323.
(8) Kruger, H.; Lutz, O.; Nolle, A.; Schwenk, A. *Z. Phys. A* **1975**, *273*, 325.
(9) Webb, G. A. "NMR and the Periodic Table"; Harris, R. K., Mann, B. E., Eds.; Academic Press: London, 1978; Chapter 3.

Table II. Calculated ^{199}Hg NMR Intensities and Frequencies of the Hg_3^{2+} Cation at 44.80 MHz[a]

isotopic isomer	spin syst	assignt	transition no.[b]	freq, Hz[c]	rel intens
$[^{199}Hg\text{-}Hg\text{-}Hg]^{2+}$		T		−43 270[d]	1.000
$[Hg\text{-}^{199}Hg\text{-}Hg]^{2+}$		C		−88 140[d]	0.500
$[^{199}Hg\text{-}Hg\text{-}^{199}Hg]^{2+}$		T		−43 270[d]	0.203
$[^{199}Hg\text{-}^{199}Hg\text{-}Hg]^{2+}$	AB	T	1	77 500	0.004 86
			2	−62 200[d]	0.198
		C	3	−69 200[d]	0.198
			4	−208 900	0.004 86
$[^{199}Hg\text{-}^{199}Hg\text{-}^{199}Hg]^{2+}$	AB_2	T	8	131 000	0.000 041
			7	−28 600	0.001 22
			6	−56 200[d]	0.003 56
			5	−57 900[d]	0.004 74
		C	4	−60 500[d]	0.003 55
			3	−88 140	0.001 20
			2	−250 000	0.000 017
			1	−277 000	0.000 031
		comb.	9	163 000	0.000 007 3

[a] Data reported for $Hg_3^{2+}(AsF_6^-)_2$ in SO_2 solvent at −70 °C with use of $J_{^{199}Hg\text{-}^{199}Hg}$ = 139 700 Hz and the observed chemical shifts of the terminal and central mercury atoms. [b] The numbering schemes used to denote the individual transitions of the AB and AB_2 spin systems are those given in ref 7. [c] Frequencies are with respect to liquid $(CH_3)_2Hg$ at 24 °C. [d] Lines observed in this work.

observed transition energies of the AB spin system and the peak positions corresponding to isotopic isomers ^{199}Hg–Hg–Hg, Hg–^{199}Hg–Hg, and ^{199}Hg–Hg–^{199}Hg, values of 139 700 ± 300 and 139 600 ± 1000 Hz were obtained for $^1J_{^{199}Hg\text{-}^{199}Hg}$, with use of data obtained at 44.80 MHz (5.872 T) and 16.08 MHz (2.114 T), respectively. No attempt was made to find the other resonances (transitions 1 and 4) arising from the AB spin system as these lines have an intensity that is ~2% of the intensity of either transition 2 or 3 and would be expected at approximately 140 kHz on either side of transitions 2 and 3 (Table II). Three weak resonances were also observed (Figure 1b) corresponding to the very small concentration (0.48%) of Hg_3^{2+} present in solution with all three nuclei as ^{199}Hg. These weak resonances correspond to transitions 4, 5, and 6 of an AB_2 spin system (numbering scheme given in ref 10, see Table II). The remaining six transitions are either too weak to be observed or are coincident with the resonance of Hg–^{199}Hg–Hg (transition 3). The calculated relative intensities and frequencies of all the peaks observed are summarized in Table II.

Spectra were also obtained for Hg_3^{2+} in HSO_3F solvent. Again, spectra were not observed at room temperature, but at −60 °C spectra similar to that obtained in SO_2 were obtained (Figure 1). However, the chemical shifts were slightly different in HSO_3F solvent. This difference may be attributed to changes in solvent diamagnetism. The Hg–Hg coupling constant was in agreement with that obtained for $Hg_3(AsF_6)_2$ in SO_2 ($J_{^{199}Hg\text{-}^{199}Hg}$ = 139 600 ± 1000 Hz) although the peaks were broader. Another resonance, assigned to Hg_2^{2+}, was always present in HSO_3F solutions of Hg_3^{2+} and is the result of oxidation of Hg_3^{2+} by the solvent.

Exchange processes are clearly observed in SO_2 solutions of Hg_3^{2+}. Some exchange may also occur in solutions of Hg_2^{2+}, but as Hg_2^{2+} has only one resonance, no signal broadening is observed. With Hg_3^{2+}, any exchange process interchanges the middle and terminal mercury atoms; hence these peaks broaden on raising the temperature.

Hg_4^{2+}. The ^{199}Hg spectrum of Hg_4^{2+} consisted of a broad, featureless resonance at −1312 ppm at room temperature ($w_{1/2}$ = 1900 Hz). When the sample was cooled to −60 °C the resonance became too broad to observe. Further cooling to −70 °C produced no discernible resonances. As noted earlier, Hg_4^{2+} solutions contain considerable amounts of Hg_3^{2+}. This would presumably allow for a very facile exchange of a terminal mercury on Hg_4^{2+} with Hg_3^{2+} according to equilibrium 2. The Raman spectra[2] of Hg_4^{2+} solutions show bands as-

$$*Hg_4^{2+} + Hg_3^{2+} \rightleftharpoons [*Hg_3^{2+}\cdots *Hg\cdots Hg_3^{2+}] \rightleftharpoons *HgHg_3^{2+} + *Hg_3^{2+} \rightleftharpoons \text{etc.} \quad (2)$$

signable to Hg_3^{2+} down to the freezing point of SO_2 (ca. −70 °C). ^{199}Hg resonances due to Hg_3^{2+} are not observed in our spectra, even at low temperatures. This is consistent with the conclusion that there are exchange processes in SO_2 solutions containing Hg_4^{2+}.

Hg–Hg Coupling Constant in Hg_3^{2+}. The large isotropic coupling constant $^1J_{^{199}Hg\text{-}^{199}Hg}$ is due to two main factors: (1) the mercury valence orbitals are predominately 6s in character, and (2) the 6s electron density at the mercury nucleus is large due to relativistic effects on this heavy nucleus. Both of these factors contribute to the dominant Fermi contact term for spin–spin coupling. Santry and Pople[11] have derived an approximate form of the theory for the Fermi contact term using the LCAO approximation, in terms of a reduced coupling constant K_{AB}

$$K_{AB} = \frac{J_{AB}4\pi^2}{h\gamma_A\gamma_B} \quad (3)$$

$$K_{AB} = {}^4/_9\mu_0^2\mu_B^2[S_A^2(0)][S_B^2(0)]\Pi_{AB} \quad (4)$$

where $S_A^2(0)$ and $S_B^2(0)$ are the valence shell s-atomic orbital densities centered on nuclei A and B, respectively, and Π_{AB} is a "mutual polarizibility" term

$$\Pi_{AB} = 4\sum_{i}^{occ}\sum_{j}^{unocc}(\epsilon_i - \epsilon_j)^{-1}C_{iA}C_{iB}C_{jA}C_{jB} \quad (5)$$

The C terms are the coefficients in the LCAO approximation and $\epsilon_i - \epsilon_j$ is the excitation energy difference between an occupied and an unoccupied MO. The reduced coupling constant calculated for Hg_3^{2+} is $^1K_{Hg\text{-}Hg} = 3.660 \times 10^{24}$ N A^{-2} m^{-3}.

Kleier and Wadt[12] have reported the results of an ab initio generalized valence-bond calculation using a relativistic effective core potential for the mercurous halides Hg_2F_2 and Hg_2Cl_2. They found the HOMO was mainly of s character, the p character being ~30% in both cases. Relativistic cal-

(10) Emsley, J. W.; Feeney, J.; Sutcliffe, L. H. "High Resolution Nuclear Magnetic Resonance Spectroscopy"; Pergamon Press: London, 1965; Vol. 1, Chapter 8.

(11) Pople, J. A.; Santry, D. P. *Chem. Phys. Lett.* **1967**, *1*, 465.
(12) Kleier, D. A.; Wadt, W. R. *J. Am. Chem. Soc.* **1980**, *102*, 6909.

culations for Au_2,[13] which is isoelectronic with Hg_2^{2+}, also show mainly 6s character for the HOMO. In order to do an order of magnitude calculation for the coupling constant, we have used the LCAO approximate theory of Pople and Santry[11] for the contact term with a basis set consisting of the 6s atomic orbitals of the mercury atoms. With use of a simple Hückel treatment by the neglect of overlap integrals and consideration of bond orbitals only between adjacent AO's, this generates three molecular orbitals

$$\sigma_g = (1/2)\phi_A + (1/2^{1/2})\phi_B + (1/2)\phi_C$$
$$\sigma_u = (1/2^{1/2})\phi_A - (1/2^{1/2})\phi_C \quad (6)$$
$$\sigma_g^* = (1/2)\phi_A - (1/2^{1/2})\phi_B + (1/2)\phi_C$$

where σ_g and σ_u are doubly occupied and are bonding and nonbonding orbitals, respectively, and σ_g^* is an empty antibonding orbital. ϕ_A and ϕ_C are the 6s atomic orbitals centered on the terminal mercury atoms, and ϕ_B is the 6s atomic orbital centered on the central mercury atom.

There is a strong UV absorption for Hg_3^{2+} at 325 nm that tails into the visible region, giving Hg_3^{2+} its characteristic yellow color.[5] We have assigned this transition to $\sigma_u \rightarrow \sigma_g^*$. The only excitation that contributes to K_{AB} is from $\sigma_g \rightarrow \sigma_g^*$, since σ_u contains a node. The excitation energy $(\epsilon_i - \epsilon_j)$ is then about twice the energy of the $\sigma_u \rightarrow \sigma_g^*$ transition.

Pyykkö has calculated[14] the value of the hyperfine integral, ν_{-1}, related to $S^2(0)$ by eq 7, for Hg^+ and Hg by a relativistically parameterized extended Hückel method. For mercury in Hg_3^{2+} we used an average of the ν_{-1} hyperfine integrals for Hg and Hg^+ to calculate an $S^2(0)$ of $43.6a_0^{-3}$.

$$S^2(0) = \frac{-137}{2\pi}\nu_{-1}a_0^{-3} \quad (7)$$

From the approximate theory for the Fermi contact term we have calculated $^1J_{^{199}Hg-^{199}Hg}$ to be 80 000 Hz, compared with 139 700 Hz for the experimental value. The difference between the experimental value and the calculated value may be due to the approximate nature of the MO's, to the neglect of electron correlation inherent in the MO approximation, and possibly to an incorrect assignment of the observed electronic transition. However, it is worth noting that, with use of a nonrelativistic theoretical calculation to obtain $S^2(0)$, the calculated value for $^1J_{Hg-Hg}$ would be one order of magnitude smaller.

The bonding in HD is very similar to that in Hg_2^{2+} since the HOMO and LUMO of HD are mostly s character. A rough order of magnitude comparison can be made between Hg_3^{2+} and HD by defining a "reduced density" coupling constant, L_{AB}:

$$L_{AB} = \frac{K_{AB}}{[S_A^2(0)][S_B^2(0)]} \quad (8)$$

In this case for HD, using the value $J_{HD} = 43.5$ Hz,[15] we obtained $L_{HD} = 1.71 \times 10^{-41}$ N A^{-2} m^3, which is comparable to $L_{Hg-Hg} = 4.2 \times 10^{-41}$ N A^{-2} m^3 for Hg_3^{2+}. The major difference between these values is due to the larger excitation energies, $\epsilon_i - \epsilon_j$, for HD and differences in the LCAO coefficients. For Hg_2^{2+}, the excitation energy $\sigma_g \rightarrow \sigma_u^*$ is smaller than for Hg_3^{2+} and the product of the coefficients $C_{iA}C_{iB}C_{jA}C_{jB}$ evaluated for Hg_2^{2+} is $^1/_4$ and that for Hg_3^{2+} is $^1/_8$. Thus, we expect the coupling constant to be substantially larger for Hg_2^{2+} than for Hg_3^{2+}. The calculation again illustrates that the large Hg–Hg coupling constant of Hg_3^{2+} is due primarily to relativistic effects. Pyykkö[16] has recently listed relativistic (and nonrelativistic) hyperfine integrals for the main-group elements that seem to be particularly appropriate for comparing homologous series of compounds, such as the group 5 hexafluoride anions. In a previous paper[17] we reported the anomalously high value for K_{Bi-F} in BiF_6^- as compared to those for its group 5 congeners using a model developed by Reeves.[18] Comparison of the "reduced density" coupling constant for this series however shows that L_{Bi-F} is smaller than for any of its congeners. This again illustrates the care needed in comparing coupling constants involving heavy elements with those involving lighter elements.

Experimental Section

Materials. Commercial liquid SO_2 (Canadian Liquid Air) was dried over P_2O_5 prior to use. Fluorosulfuric acid (J. T. Baker) was purified by the standard literature methods.[19] Triply distilled mercury (Canlab), HgO (J. T. Baker), 70% $HClO_4$, (British Drug House), HgF_2 (Ozark-Mahoning), AsF_5 (Ozark-Mahoning), and $(CH_3)_2Hg$ (Ventron) were used without further purification.

The preparations of $Hg_2(AsF_6)_2$, $Hg_3(AsF_6)_2$, $Hg_4(AsF_6)_2$, and $Hg_3(Sb_2F_{11})_2$ have been described elsewhere.[20]

$Hg(AsF_6)_2$ was prepared by condensing a 10% excess of AsF_5 into a previously dried and evacuated ampule containing HgF_2 and SO_2 at −196 °C. The vessel was outfitted with a $^1/_4$ in. glass tube and connected to the vacuum line by means of a Teflon valve and $^1/_4$ in. Teflon compression fittings. The vessel was sealed by closing the Teflon valve, warmed to room temperature, and stirred by means of a magnetic stirbar until dissolution of HgF_2 was complete. The SO_2 was then removed under vacuum at room temperature and the remaining solid used without further purification.

A solution of $Hg_3(SO_3F)_2$ in HSO_3F was prepared in a dry glass ampule (see above) joined, by means of a glass frit, to a 10 mm o.d. precision NMR tube (Wilmad). Mercury was stirred vigorously at room temperature with HSO_3F for 12 h. The resultant light yellow solution was then filtered through the glass frit into the NMR tube, which was sealed under vacuum at −196 °C. The NMR spectrum was recorded within 1 day of sample preparation as additional oxidation occurs to form the less soluble $Hg_2(SO_3F)_2$ compound.

$Hg(ClO_4)_2$ was prepared by dissolving HgO in concentrated $HClO_4$, and NMR samples were prepared by diluting this stock solution.

$Hg_2(ClO_4)_2$ was prepared as previously described[21] by stirring mercury with an aqueous solution of $Hg(ClO_4)_2$. NMR samples were prepared directly from these solutions.

Sample Preparations. NMR samples in SO_2 solvent were prepared by transferring the appropriate solid in a drybox into a dry thin-wall 10 mm o.d. NMR tube fitted with a Teflon valve and compression fittings (see above). The tube was evacuated and SO_2 condensed onto the solid at −196 °C. The tube was then sealed off under vacuum and warmed under a tepid stream of water until some SO_2 had liquefied, at which point the tube was left to warm to room temperature.

Nuclear Magnetic Resonance Spectroscopy. Mercury-199 NMR spectra were recorded at 44.800 MHz on a Bruker WM-250 superconducting spectrometer. A low-field spectrum of Hg_3^{2+} was also obtained at 16.079 MHz with a Bruker WH-90 spectrometer. The 44.800-MHz spectra were recorded unlocked (field drift < 0.1 Hz/h) with use of a spectral width of 100 kHz (32K memory size, 6.1 Hz/data point; acquisition time 0.16 s) and a ~90° pulse of 20 μs. The 16.079-MHz spectrum of Hg_3^{2+} was obtained with use of an external D_2O lock mounted within the probe head, a spectral width of 35.7 kHz (16K memory size, 4.4 Hz/data point; acquisition time 0.23 s), and a ~90° pulse of 25 μs. Approximately 50 000–70 000

(13) (a) Ermler, W. C.; Lee, Y. S.; Pitzer, K. S.; McLean, A. D. *J. Chem. Phys.* **1979**, *70*, 288. (b) Ermler, W. C.; Lee, Y. S.; Pitzer, K. S. *Ibid.* **1979**, *70*, 293.
(14) Jokisaari, J.; Ralsanen, K.; Kuonanoja, J.; Pyykkö, P.; Lajunen, L. *Mol. Phys.* **1980**, *39*, 715.
(15) Cour, Y. H.; Purcell, E. M. *Phys. Rev.* **1952**, *88*, 415.
(16) Pyykkö, P.; Wiesenfeld, L. *Mol. Phys.* **1981**, *43*, 557.
(17) Morgan, K.; Sayer, B. G.; Schrobilgen, G. J. *J. Magn. Reson.* **1983**, *52*, 139.
(18) (a) Reeves, L. W. *J. Chem. Phys.* **1964**, *40*, 2128. (b) Reeves, L. W. *Ibid.* **1964**, *40*, 2132. (c) Reeves, L. W. *Ibid.* **1964**, *40*, 2423. (d) Inglefield, P. T.; Reeves, L. W. *Ibid.* **1964**, *40*, 2424.
(19) Barr, J.; Gillespie, R. J.; Thompson, R. C. *Inorg. Chem.* **1964**, *3*, 1149.
(20) Cutforth, B. D.; Gillespie, R. J. *Inorg. Synth.* **1979**, *19*, 22.
(21) Newbery, E. *Trans. Electrochem. Soc.* **1936**, *69*, 611.

free induction decays were accumulated for Hg_3^{2+} and Hg_4^{2+} spectra recorded at 44.800 MHz and ca. 5000 for all other spectra. The decays were smoothed before being transformed into the frequency domain with use of a line-broadening parameter of 20 Hz for Hg_3^{2+} and Hg_4^{2+} at 44.800 MHz and 3-6 Hz for all other spectra.

Both spectrometers were equipped with variable-temperature controllers. The reported temperatures were measured by inserting a copper-constantan thermocouple directly into the probe and are accurate to ±1 °C.

Acknowledgment. We wish to thank Dr. D. P. Santry for useful discussions, the Natural Sciences and Engineering Research Council of Canada for financial support, and the Canada-France Exchange Program (administered jointly by the NSERC, Ottawa, Canada, and the CNRS, Paris, France) for a travel and subsistence grant to P.G.

Registry No. Hg^{2+}, 14302-87-5; Hg_2^{2+}, 12596-26-8; Hg_3^{2+}, 12596-27-9; Hg_4^{2+}, 51383-32-5; ^{199}Hg, 14191-87-8.

Contribution from the Department of Chemistry, The American University, Washington, D.C. 20016

pK_a and Isomer Determinations of Cobalt(III) Imidazole and Histidine Complexes by NMR and X-ray Crystallography

N. R. BRODSKY,[1a] N. M. NGUYEN,[1a] N. S. ROWAN,*[1a] C. B. STORM,[1b] R. J. BUTCHER,[1b] and E. SINN[1c]

Received September 30, 1982

The pK_a's for *cis*-$Co(en)_2(H_2O)ImH^{3+}$, *cis*-$Co(en)_2(H_2O)(N\text{-MeIm})^{3+}$, *cis*-$Co(en)_2(H_2O)(4\text{-MeImH})^{3+}$, and $Co(en)(H_2O)HisH^{2+}$ are 5.85, 5.95, 5.95, and 6.20 for pK_{a_1}, respectively, at 25 °C and 10.5, ..., 10.8, and 10.8 for pK_{a_2}, respectively, as determined by potentiometric titration and ^1H NMR spectroscopy. pK_{a_1} represents the water ionization and pK_{a_2} the imidazole ionization. Changes in chemical shift for the acidic and basic forms of the coordinated imidazole were 0.6 ppm for the C(2)-H, 0.25 ppm for the C(4)-H, and about 0.16 ppm for the C(5)-H, which were similar to the changes found in $Co(NH_3)_5ImH^{3+}$. ^1H NMR titration behavior showed that the histidine was coordinated through an imidazole nitrogen, and ^{13}C NMR spectra indicated that this is N1. The single-crystal X-ray structure determination of the coordination environment of the complex showed that the histidine is tridentate. Crystal data for [Co(HisH)(en)Cl]Cl: space group $P\bar{1}$, $Z = 2$, $a = 7.939$ (2) Å, $b = 9.247$ (3) Å, $c = 11.021$ (4) Å, $\alpha = 118.75$ (3)°, $\beta = 97.76$ (3)°, $\gamma = 97.72$ (2)°, $R = 3.7\%$ for 3533 reflections. ^{13}C spectra also indicated the methyl group in the 4-methylimidazole complex was adjacent to the ionizable hydrogen. Changes in ligand, charge of the complex, substituents on the imidazole ring, and geometry of the complex all changed the C(2)-H chemical shift about 0.1 ppm. Ionization of coordinated water changed the C(2)-H chemical shift of coordinated imidazole less than 0.1 ppm and had less effect on the C(4)-H and C(5)-H resonances. Slow C(2) hydrogen exchange was found at pH 10.6 for *cis*-$Co(en)_2(OH)Im^+$. More rapid C(2)-H exchange was found for *cis*-$Co(en)_2(OH)(N\text{-MeIm})^{2+}$ at pH 12. In both cases the rates were slower than for the analogous methylated or protonated species.

Introduction

Histidine, the amino acid containing the aromatic side chain imidazole, is important in binding metal ions to proteins. NMR methods have been used to identify individual residues and determine which histidines are coordinated to metal ions.[2-4] In many cases it is difficult to tell whether an unusual imidazole pK_a is due to coordination or environmental effects. Because of our interest in coordinated imidazole, we used substitution-inert model complexes to examine some of the properties of coordinated imidazoles. In our model complexes, ligand changes, charge changes, geometry changes, pH titration behavior, C2-H exchange, and substitution effects could all be evaluated without the possibility of interference from environment effects.[3] In our studies we used *cis*-$Co(en)_2ClImH^{2+}$, *cis*-$Co(en)_2Cl(N\text{-MeIm})^{2+}$, *cis*-$Co(en)_2Cl(4\text{-MeImH})^{2+}$, $Co(en)ClHisH^+$ and their hydrolysis products in acidic and basic solution (en = ethylenediamine, Me = methyl, ImH = neutral imidazole, HisH = $NH_2CH(COO)CH_2ImH$). The aquated complexes contained a water molecule and an imidazole coordinated to the same metal center. The Zn^{2+} in carbonic anhydrase is coordinated to three histidines and a water molecule. An ionization occurs at pH 6-7, which is necessary for the catalytic reaction, but the mechanism for the reaction is not well understood.[5,6] Whether this ionization is due to a coordinated H_2O or coordinated histidine or some group in the cavity nearby is not known although recent evidence in the Co(II) enzyme shows that no imidazole N-H's are lost.[7] In the studies of the model complexes it was possible to observe the change in C(2)-H resonance during both the H_2O ionization and the imidazole ionization.

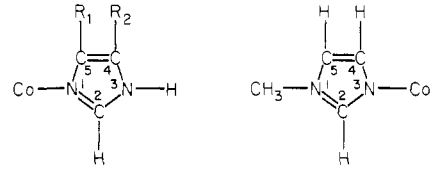

ligands:
imidazole (R_1, R_2 = H),
histidine (R_1 = $-CH_2CH(NH_2)$-(COOH), R_2 = H),
4-methylimidazole
(R_1 = H, R_2 = CH_3)

Experimental Section

Synthesis. *cis*-$[Co(en)_2ClImH]Cl_2$, *cis*-$[Co(en)_2Cl(N\text{-MeIm})]Cl_2$, and *cis*-$[Co(en)_2Cl(4\text{-MeImH})]Cl_2$ were all synthesized by the method of Kindred and House.[8] The complexes were recrystallized from a

(1) (a) The American University. (b) Present address: the Department of Chemistry, Howard University, Washington, DC 20059. (c) Present address: Department of Chemistry, University of Virginia, Charlottesville, VA 22901.
(2) Markley, J. L. *Acc. Chem. Res.* **1975**, *8*, 70.
(3) Cass, A. E. G.; Hill, H. A. O.; Bannister, J. V.; Bannister, W. H.; Hasemann, V.; Johansen, J. T. *Biochem. J.* **1979**, 127.
(4) Allerhand, A. *Acc. Chem. Res.* **1978**, *11*, 469.
(5) Bertini, I.; Luchinat, C.; Scozzafava, A. *Struct. Bonding (Berlin)* **1982**, *48*, 45 and references therein.
(6) Pesando, J. M.; Gupta, R. K. *Bioorg. Chem.* **1981**, *10*, 115.
(7) Bertini, I.; Cant, G.; Luchinato, C.; Mani, F. *J. Am. Chem. Soc.* **1981**, *103*, 7784.

0020-1669/84/1323-0891$01.50/0